Experimental Data for Particle Deposition in Turbulent Flows

Extensive reviews of the experimental data for particle deposition in a vertical duct were reported by McCoy and Hanratty (1977) and Papavergos and Hedely (1984). The trend of the experimental data is shown in Figure 1. For very small particles, the Brownian motion significantly affects the deposition rate and the deposition velocity increases as particle relaxation time (diameter) decreases. The minimum deposition velocity occurs in the range of $10^{-2} < \tau^+ < 5\times10^{-1}$. For larger particles, the deposition velocity increases rapidly with the relaxation time up to $\tau^+ \approx 20$, and then saturates to a constant value of about 0.18. For a vertical duct flow, Papavergos and Hedely (1984) suggested

$$u_D^+ = 0.065 S_c^{-2/3} \quad \text{for} \quad \tau^+ < 0.2 \tag{1}$$

$$u_D^+ = 3.5\times10^{-4}\tau^{+2} \quad \text{for} \quad 0.2 < \tau^+ < 20 \tag{2}$$

$$u_D^+ = 0.18 \quad \text{for} \quad \tau^+ > 20 \tag{3}$$

In Figure 1 the prediction of the modified version of Papavergos and Hedely (1984) equation given by

$$u_D^+ = 0.065 S_c^{-2/3} + 3.5\times10^{-4}\tau^{+2} \quad \text{for} \quad \tau^+ < 20 \tag{4}$$

is compared with the experimental data. Here a shear velocity of 0.3 m/s and a density ratio of 2000 is assumed. The model of Fan and Ahmadi (1993) is also shown in this figure for comparison. It is seen that the model predictions are in good agreement with the data.

For a horizontal duct, Papavergos and Hedely (1984) suggested

Floor Deposition

$$u_D^+ = 2\times10^{-3}\tau^{+2} \quad \text{for} \quad 0.2 < \tau^+ < 20 \tag{5}$$

Ceiling Deposition

$$u_D^+ = 4\times10^{-5}\tau^{+2} \quad \text{for} \quad 0.2 < \tau^+ < 20 \tag{6}$$

The model predictions of Equations (5) and (6) modified by addition of the Brownian deposition term are shown in Figure 2. It is seen that the model predictions are in reasonable agreement with the trend of the experimental data.

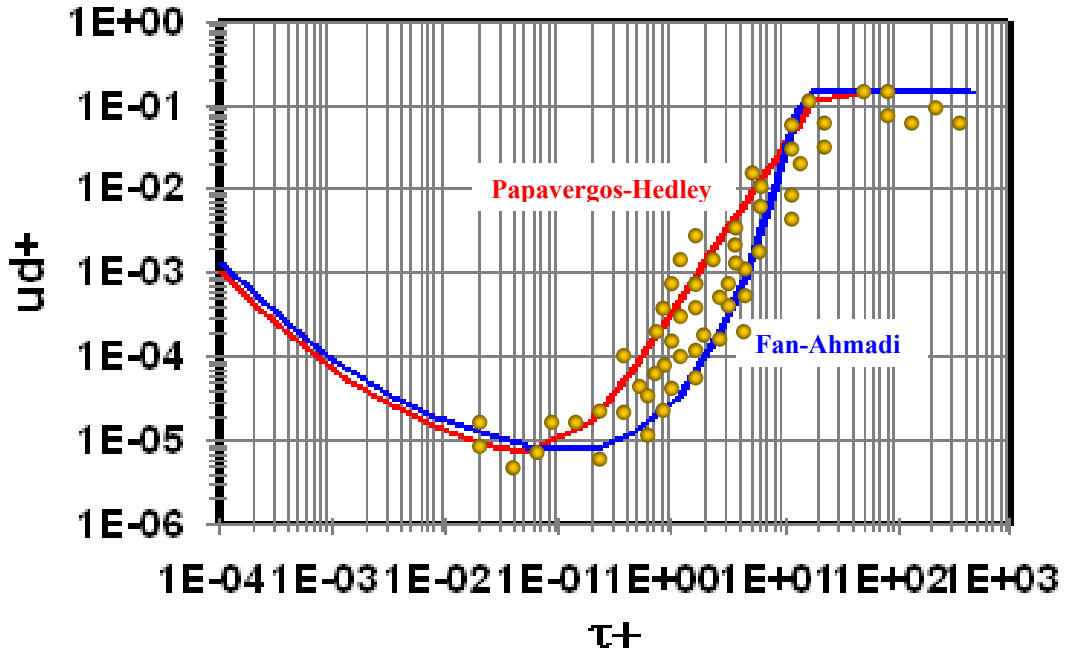

Figure 1. Comparison of the model predictions with the trend of experimental data for a vertical duct.

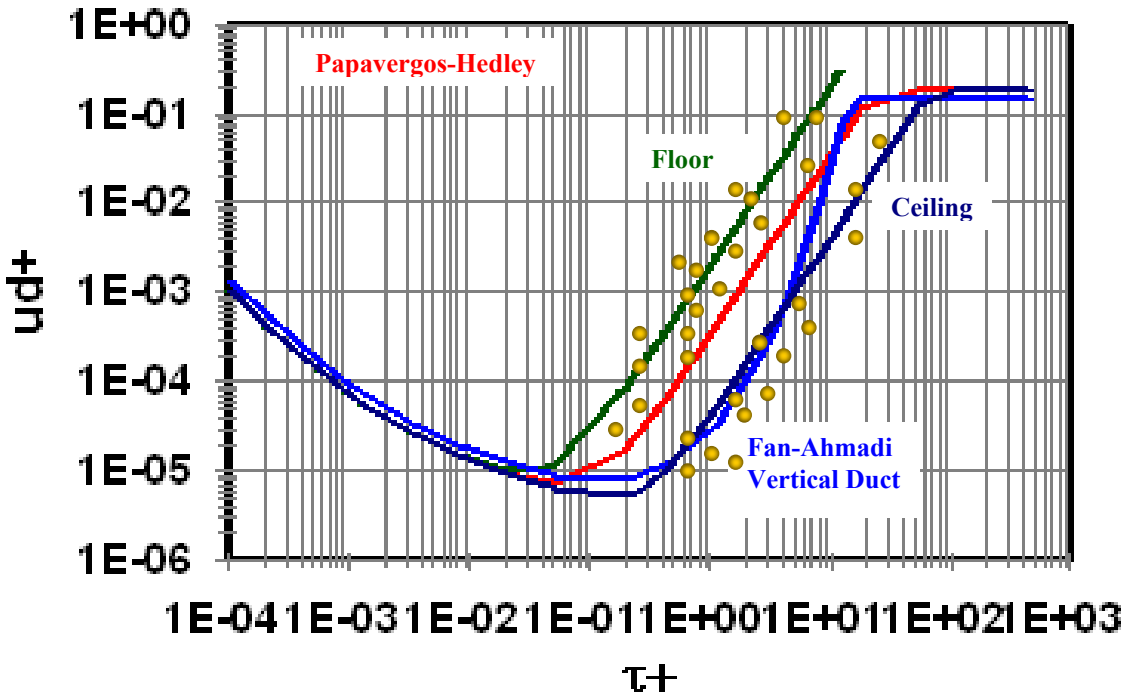

Figure 2. Comparison of the model predictions with the trend of experimental data for a horizontal duct.

While the empirical equations appear to provide reasonable fits to the data, they are limited in that they do not account for the effects of density ratio $S = \rho^p / \rho^f$, flow Reynolds number, or spectral characteristic of turbulence.

Summary of Classical Turbulence Deposition Models

Near a wall, the particle mass flux is given by

$$J = (D + D^T)\frac{\partial C}{\partial y} \tag{7}$$

where D and D^T are Brownian and turbulent particle diffusitivities. In terms of wall units, Equation (7) may be restated as

$$u_D^+ = (D^+ + D^{T+})\frac{\partial C^+}{\partial y^+}, \qquad D^+ = S_c^{-1} \tag{8}$$

where the non-dimensional deposition velocity is defined as

$$u_D^+ = \frac{u_D}{u^*} = \frac{1}{u^*}\left(\frac{J}{C_0}\right) \tag{9}$$

and

$$C^+ = \frac{C}{C_0}, \tag{10}$$

where C_0 is the bulk concentration. In most earlier theories, it was assumed that

$$D^T = \nu^T, \qquad D^{T+} = \nu^{T+}. \tag{11}$$

Friedlander and Johnstone Model (Free Flight)

The earliest model for turbulent deposition was reported by Friedlander and Johnstone (1957). Their key assumptions were

a)

$$D^{T+} = \nu^{T+} = \begin{cases} (\frac{y^+}{14.5})^3 & 0 < y^+ \le 5 \\ \frac{y^+}{5} - 0.959 & 5 \le y^+ \le 30 \end{cases} \tag{12}$$

b) Particles that are reaching the stopping distance from wall will deposit on the wall (free flight model). Thus, $C(s^+ + \frac{d^+}{2}) = 0$ is used as a boundary condition. Here, $s = U_f \tau$, where U_f is the particle free flight velocity and τ is the relaxation time.

a) Free flight velocity is assumed to be given by

$$U_f = 0.9u^* = 0.9\overline{U}\sqrt{\frac{f}{2}}, \quad f = C_f = \frac{\tau_0}{0.5\rho\overline{U}^2} \tag{13}$$

where f is the friction factor.

Using these assumptions, Friedlander and Johnstone (1957) found the following expressions for the deposition velocity:

$$u_d^+ = (\frac{1}{\sqrt{f/2}} + \frac{1525}{s^{+2}} - 50.6)^{-1} \quad \text{for} \quad s^+ \le 5 \tag{14}$$

$$u_d^+ = [\frac{1}{\sqrt{f/2}} - 13.75 + 5\ln(\frac{5.04}{0.5s^+ - 0.959})]^{-1} \quad \text{for} \quad 5 \le s^+ \le 30 \tag{15}$$

$$u_d^+ = \sqrt{f/2} \quad \text{for} \quad s^+ \ge 30 \tag{16}$$

where

$$s^+ = 0.9\tau^+ \tag{17}$$

The prediction of the Friedlander-Johnstone model is compared with the experimental data and other models in Figures 3-5. In Figure 5 the diffusion term is

linearly added to the model to cover the Brownian range as well. It is seen that the model well predicts the increasing trend of the deposition velocity with the particle relaxation time in the eddy impaction range.

While the model gives relatively reasonable results for the eddy impaction regime, the assumptions of free flight model with the initial velocity given by (13) are difficult to justify. In addition, Equation (16) implies that u_D^+ increases with $f\,(=0.039\,Re^{-0.17})$. Thus, u_D^+ increases with decreasing Re, which is not supported by the experimental data.

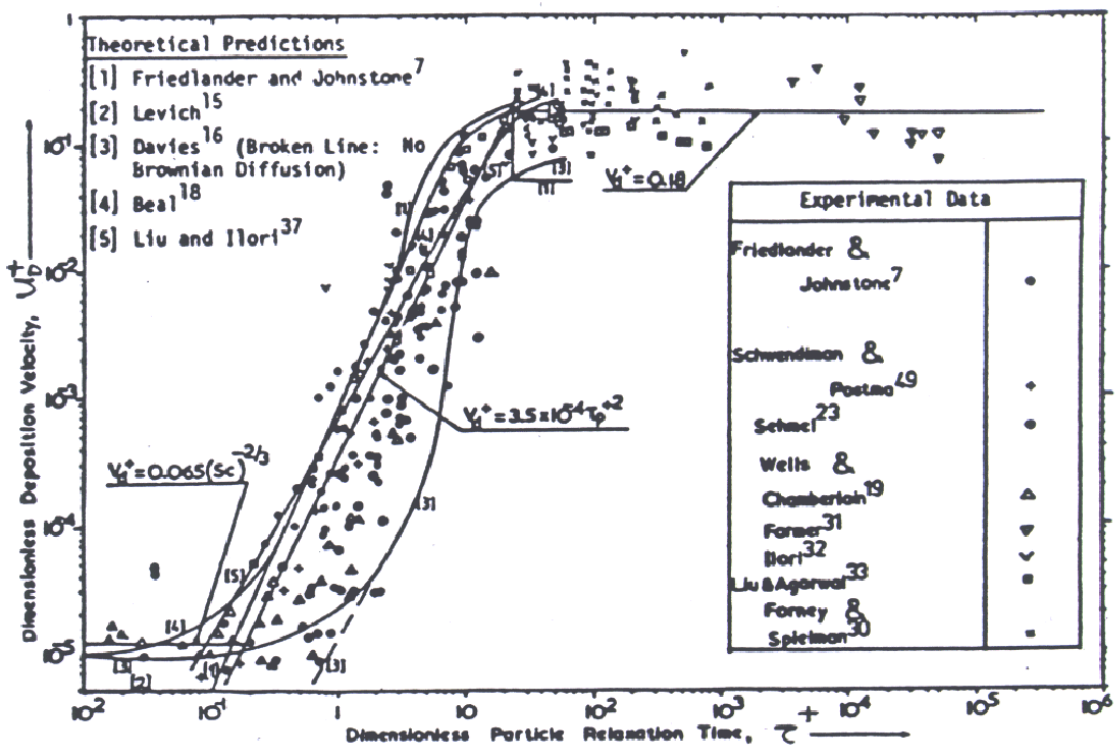

Figure 3. Comparison of the model predictions with the experimental data for a vertical duct as reported by Papvergos and Hedely (1984).

Levich Model

Levich studies the deposition of molecular size particles with $s_c >> 1$. He assumed $\nu^T \sim y^{+4}$ and found

$$u_D^+ = 0.13337 S_c^{-3/4}. \qquad (18)$$

It is now known that $\nu^T \sim y^{+3}$. The predictions of Levich's model are also shown in Figure 3-5. It is seen that the model gives reasonable results for the diffusion range.

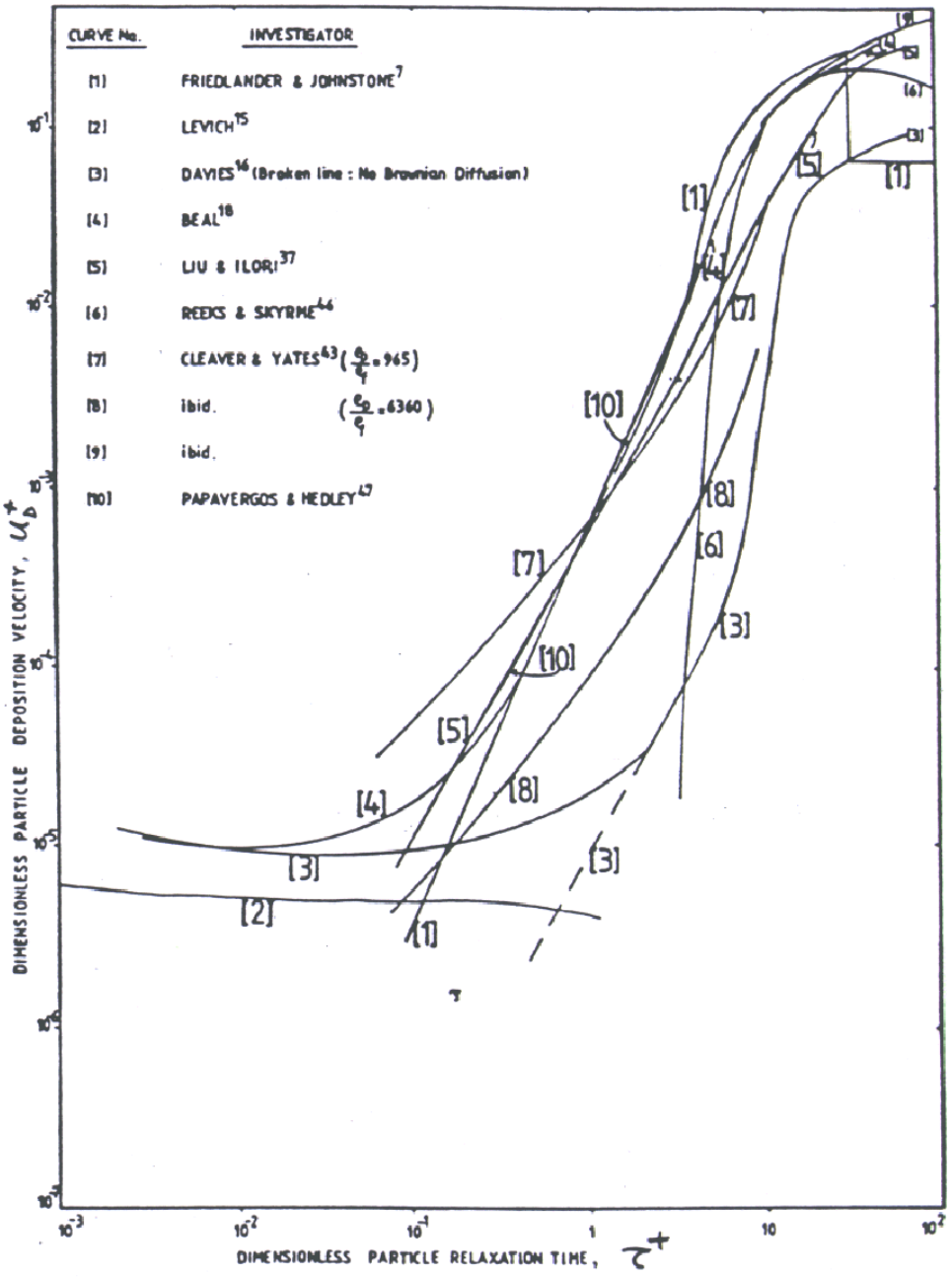

Figure 4. Comparison of different model predictions for a vertical duct as reported by Papvergos and Hedely (1984).

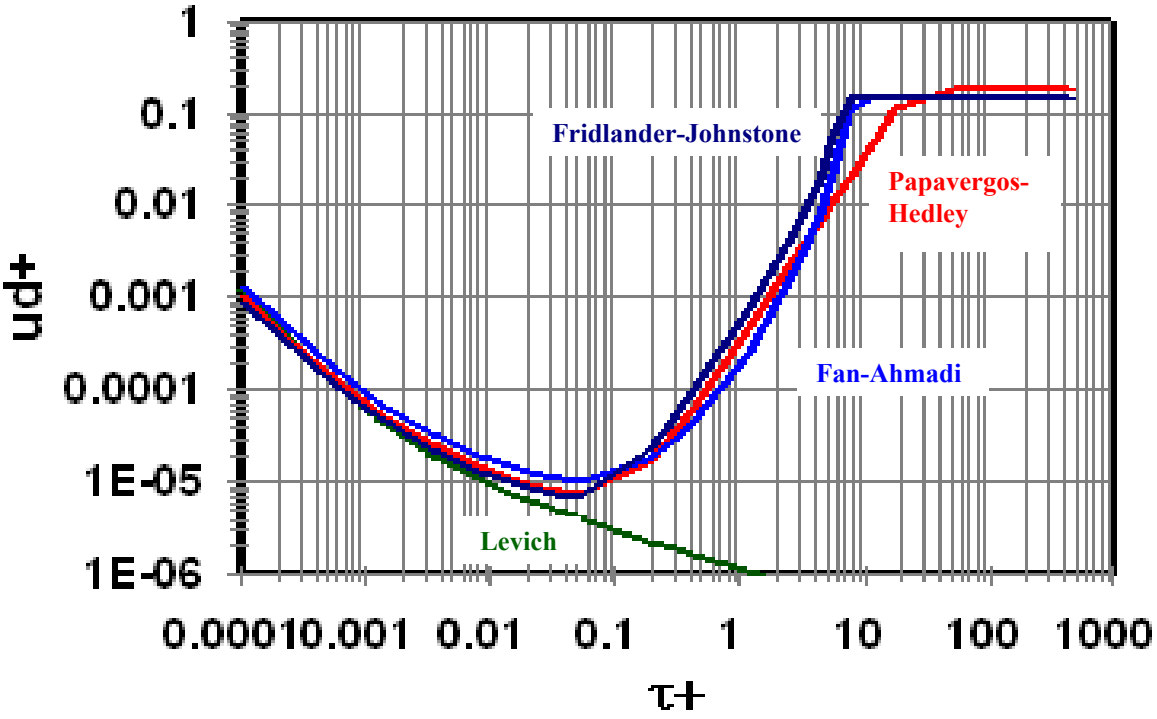

Figure 5. Comparison of different model predictions for a vertical duct for particles with a density ratio of 1000. (The diffusion term is added linearly to the models of Friedlander and Johnstone (1957) and Papvergos and Hedely (1984)).

Davies Model

For sub-micron particle, Davies found

$$u_D^+ = 0.057 s_c^{-2/3}, \tag{19}$$

which the one used in Wood's model. For $d > 1\mu$, he used an empirical expression for ν^T across the entire boundary layer and evaluated u_D^+. He also made use of stopping distance and free-flight model, however, with a more realistic local RMS fluctuation velocity as the initial free-flight velocity. Davies' model predictions are shown in Figures 3 and 4. While Davies' assumptions appear to be more realistic, his deposition velocity significantly underestimates the data.

Additional Models

There have been a number of attempts to improve the models of Friedlander and Johnstone. Beal tried to improve the agreement of Davies' approach with the experimental data. He suggested using one-half of the mean axial velocity as the initial free-flight velocity for calculating the stopping distance. He also postulated that the concentration of particles of $y^+ = s^+ + \frac{d^+}{2}$ is not zero and a continuous rate of accumulation of particles takes place in this region, which acts as an added resistance to particle wall deposition.

Sehmel used an analysis similar to Davis but employed equation of Lin et al. for eddy diffusivity. To fit the data, he found the free-flight velocity must be correlated to the particle relaxation time as

$$U_f^+ = 1.49(\tau^+)^{-0.49} \tag{20}$$

In addition, he used an empirical correlation for particle turbulent mass diffusivity as

$$\begin{aligned} D^{T+} &= 0.011(y^+)^{1.1}(\tau^+)^{1.1} \qquad y^+ < 20 \\ D^{T+} &= 0.04y^+ \qquad\qquad\qquad\quad y^+ > 20 \end{aligned} \tag{21}$$

Liu and Ilari suggested that the particle diffusivity is greater than the eddy diffusivity and is given as

$$D^{T+} = \nu^{T+} + \left(\frac{y^+}{y^+ + 10}\right)^2 \tau^+, \tag{22}$$

where coefficient of τ^+ is the estimated MS fluctuation velocity. The predictions of these different models are shown in Figures 3 and 4.

Limitations of Free-Flight Models

The class of models that are initiated with the work of Friedlander and Johnstone is referred to as the free-flight models. While the general trend of the particle deposition velocity is reasonably well predicted by these models, there are a number of limitations with the assumption used in their derivation. These are:

- Use of the concept of 'stopping distance' as a sink boundary condition for particles.

- Assumption that the free-flight velocity is equal to RMS radial fluid fluctuation velocity (or proportional to the axial velocity).
- Equality of particle mass diffusivity to the turbulence eddy diffusion.
- Ignoring the effects of density ratio, Reynolds number, and interactions with various scales of turbulence.
- Ignoring the effects of lift force.
- Ignoring the effects of coherent eddies and bursting phenomena.

Cleaver and Yates Model

It is well known that burst phenomena occur in a turbulent boundary layer. That is periodically, fluid is being ejected away from the wall and that is followed by a down-sweep and inrush of fluid toward the wall. Cleaver and Yates assumed that

- Suspended particles are able to diffuse to a certain distance from the wall by turbulent diffusion before being entrained in a down-sweep.
- The flow in a down-sweep may be approximated as a two-dimensional stagnation-point flow in the sub-layer.
- Only the Stokes drag is acting on the particles.

Their expression for the deposition velocity involves integrating over the stagnation-point velocity field. For small τ^+, a simplified expression becomes available. i.e.

$$u_D^+ = \frac{9}{400}\frac{\rho^f}{\rho^p}\tau^+ \exp\{0.48\tau^+\} + 0.084 Sc^{-2/3}, \qquad (23)$$

where the diffusion effects is also linearly added to the model.

The predictions of Cleaver and Yates' model as given by Equation (23) for density ratios of S= 500, 1000 and 2000 are shown in Figure 6 and are compared the models of Papavergos and Hedley (1984) and Fan and Ahmadi (1983) for a density ratio of 1000.

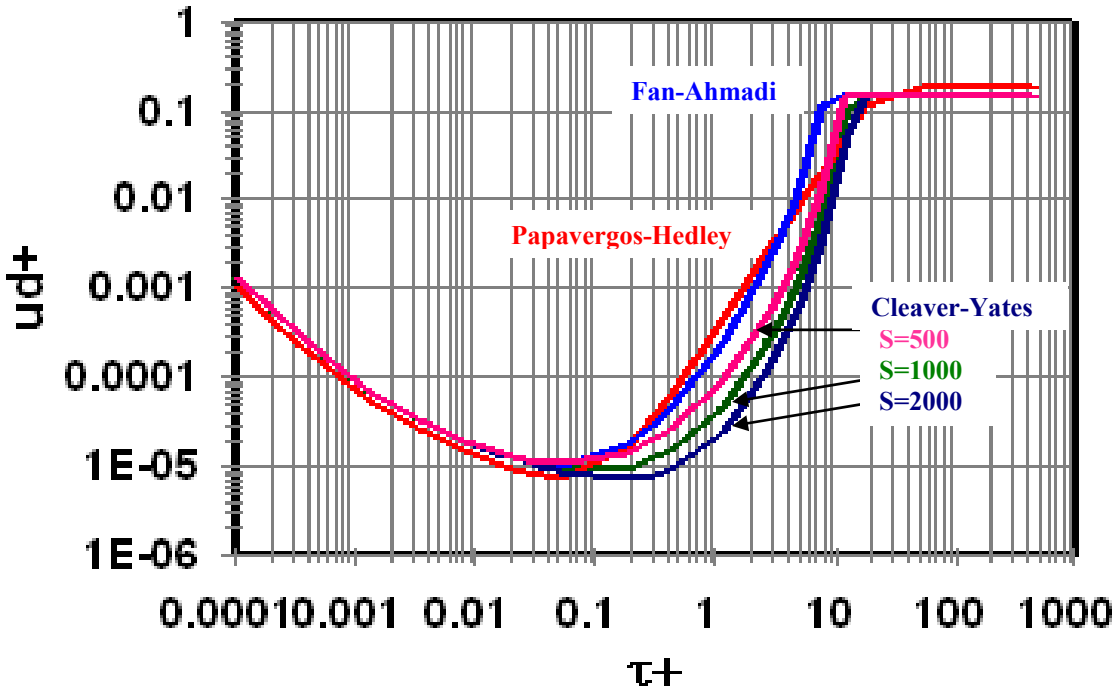

Figure 6. Comparison of model predictions of Cleaver and Yates for different density ratios with those of Papvergos-Hedely and Fan-Ahmadi.

Structure of Turbulence Near a Wall

The structure of turbulent flow near a wall and in particular in the viscous sub-layer significantly affects the deposition of particles on the wall. Certain features of turbulent flow, which have important consequences for aerosol deposition process, are described in this note.

For a low Reynolds number channel flow, turbulence intensity distributions are shown in Figure 7. It is observed that v'^{+} reaches its maximum of about 1 at $\frac{y}{b} \approx 0.2$ ($y^{+} = 40 - 50$). The maximum of u'^{+} appears a much shorter distance from the wall. The peak value here is about 2.9. However, a range of values for u'^{+}_{max} between 2.3 to 3.4 has been reported in the literature. The near wall region is also of considerable interest, since the major portion of turbulence production takes place in this region.

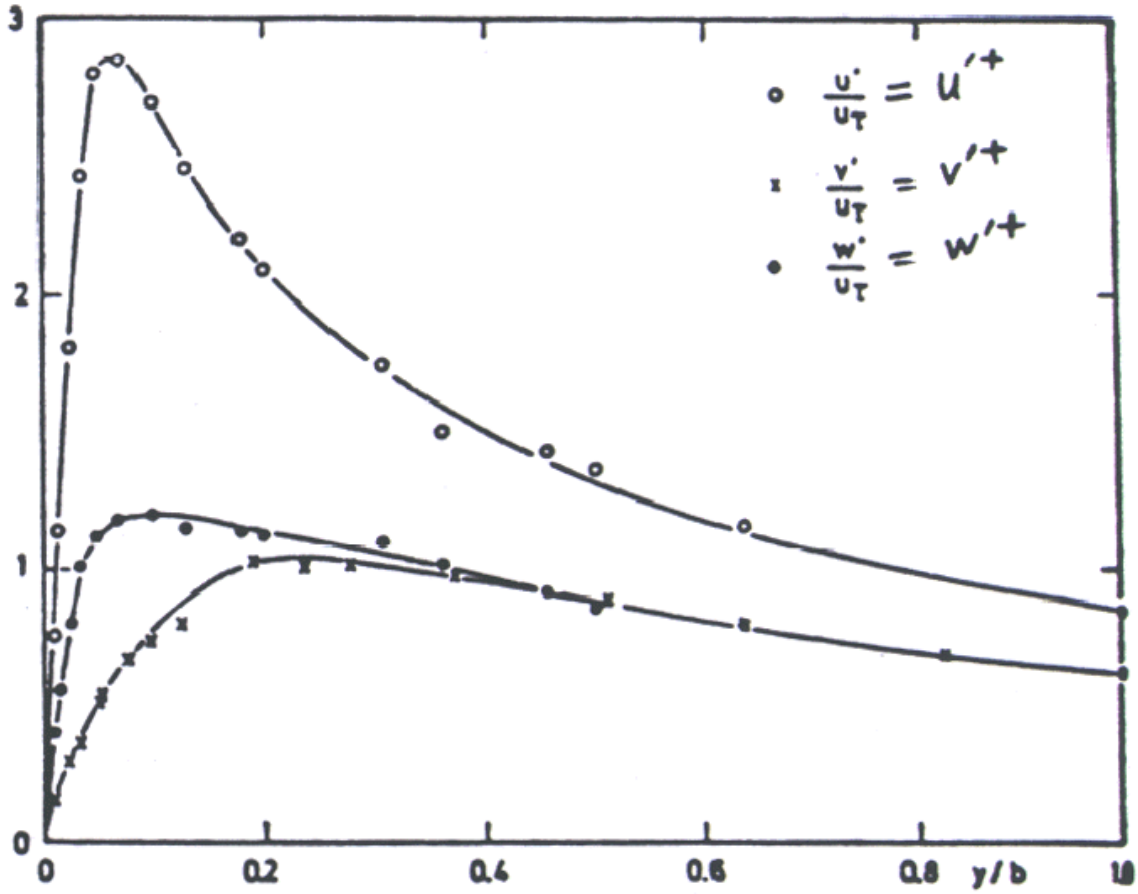

Figure 7. Variations of turbulence intensity distributions in a channel.

Streaky Nature of the Wall Flow

It is now well recognized that the viscous wall region has a fairly ordered three-dimensional structure. Flow visualization shows streaky structures in the viscous sub-layer. Low speed streaks are found to continue for large stream-wise distances of the order of 1000 wall units. The streaks have a mean spacing of about 100 wall unites which appears to be independent of the flow Reynolds number as shown in Figure 8.

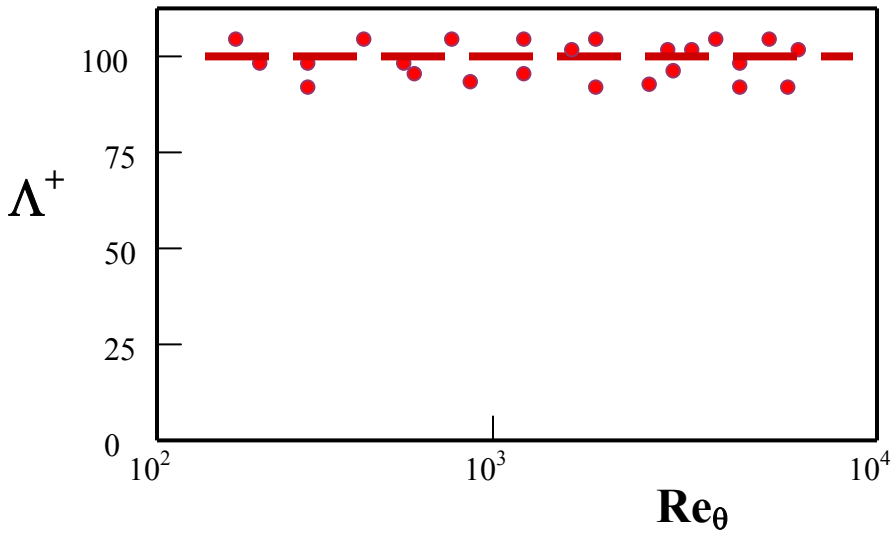

Figure 8. Variations of mean nondimensional streak spacing as function of momentum thickness Reynolds number. Comparisons with the trend of experimental data of Kline et al. (1967), Oldaket et al. (1977) and Smith et al. (1979).

The spacing is also lag-normally distributed and has a standard deviation of about 40 wall units. The streaks leave a width of 10-30 wall units and an aspect ratio of about 30 to 100. The streaks are believed to be formed by counter-rotating elongated vortices, which appear as organized structures near a wall. A schematic of the near wall eddies is shown in Figure 9.

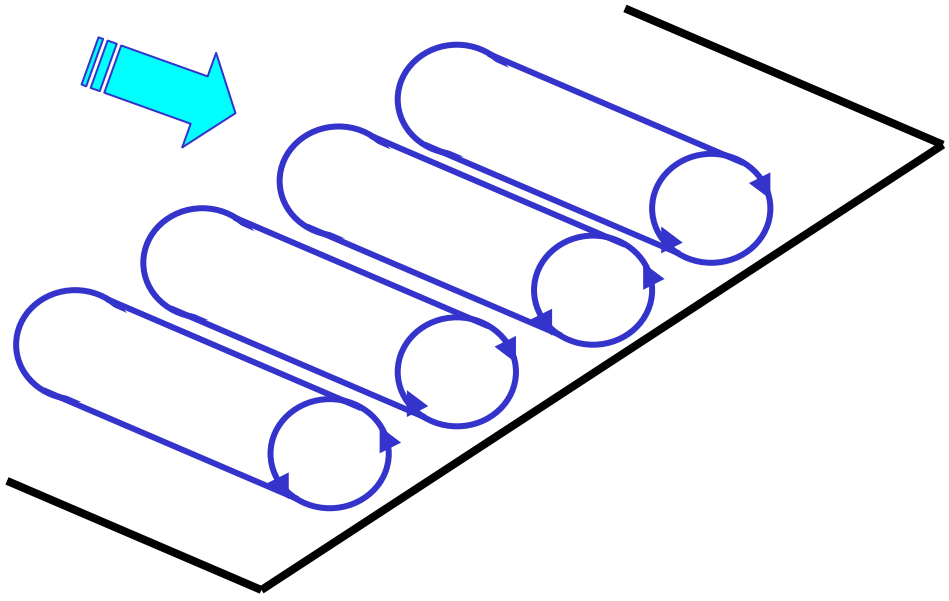

Figure 9. Schematics of near wall coherent vortices.

Bursting Phenomena

The streaks are observed to be lifted from the wall into the buffer region, which leads to an oscillating motion, which terminates in a chaotic break-up of the flow. During this quasi-periodic process, a major part of turbulence production occurs.

The lift-up produces a region of low-speed flow in the buffer zone. The instantaneous velocity profile becomes inflexional, which is highly unstable. Thus, an oscillation follows, which in turn leads to a rapid and violent mixing that is referred to as the break-up. During this phase, fluid is being ejected upward at a steep angle of about 20^o. After this chaotic phase, a "sweep" motion towards the wall at a small angle follows.

The average time between the burst T_B satisfies the following empirical equations:

$$T_B^+ = 0.65 R_\theta^{0.73}, \quad \frac{V_0 T_B}{\delta} \approx 5. \tag{24}$$

The duration of burst/sweep/inrush is roughly $0.25 T_B$.

Kline et al. hypothesized that the lift-up of the low-speed streak and the burst phenomena is associated with the formation of a horseshow vortex. The counter-rotating stream-wise vortices (with their center at $y^+ = 20 - 30$), which form the streaks, may be the legs of a horseshoe vortex. Landahl (1983) proposed a model for predicting the variation of $< u^+ >$ during a burst.

Cleaver-Yates Model (Chem. Eng. Sci. **30** (1975) 983)

Cleaver and Yates developed a model for turbulent deposition that includes the effect of near wall flow structure. A schematic of the near wall coherent eddies is shown in Figure 10. According to this model, particles with sufficient inertia will not follow the flow streamlines and impact the wall. Thus the turbulent deposition is dominated by the impaction process in the coherent wall eddies. They defined a limiting trajectory for the particles that are deposited on the wall. All particles within the limiting trajectory will deposit on the wall, while those out side the limiting trajectory will be entrained back into the core flow.

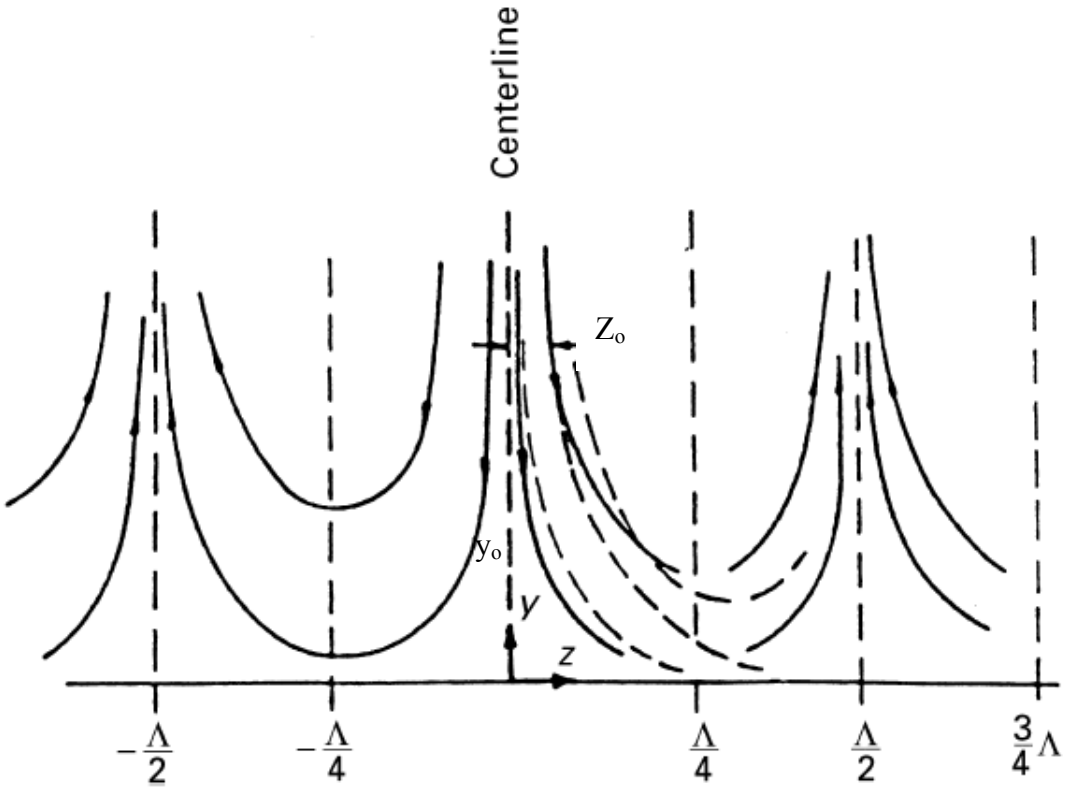

Figure 10. Schematics of near wall eddies.

The turbulent flux toward the wall is given as

$$J = C(y)v_0(y)A_c(y), \tag{25}$$

where v_0 in the RMS turbulence fluctuations perpendicular to the wall, C(y) is the concentration, and A_c is the capture area ratio (the ratio of the area between the limiting

trajectory and the centerline to the total area). The corresponding deposition velocity is given as

$$u_D^+ = \frac{J}{Cu^*} = \frac{v_0^+ A_c}{2}. \tag{26}$$

Note that the capture area ratio is given as

$$A_c - \text{capture area ratio} = \frac{z_0}{\Lambda}. \tag{27}$$

The particle trajectory in the presence of only the drag force is given as

$$\tau^+ \frac{dv^+}{dt^+} = v^{f+} - v^+, \tag{28}$$

$$\tau^+ \frac{dv^+}{dt^+} = v^{f+} - v^+, \tag{29}$$

For small particle relaxation time, τ^+, using an iterative solution and expanding the total derivative, it follows that

$$v^+ = v^{f+} - \tau^+ (v^{f+} \frac{\partial v^{f+}}{\partial y^+} + w^{f+} \frac{\partial v^{f+}}{\partial z^+}) \tag{30}$$

$$w^+ = w^{f+} - \tau^+ (v^{f+} \frac{\partial w^{f+}}{\partial y^+} + w^{f+} \frac{\partial w^{f+}}{\partial z^+}) \tag{31}$$

The down flow pattern of the near wall eddies may be modeled as plane stagnation flow. For a plane stagnation point flow,

$$w^f = \alpha z \varphi'(\eta), \qquad v^f = -\sqrt{\alpha \nu}\varphi(\eta), \qquad \eta = \sqrt{\frac{\alpha}{\nu}} y. \tag{32}$$

where φ satisfies the following equation (Schlichting, 1960):

$$\varphi''' + \varphi\varphi'' - \varphi'^2 + 1 = 0, \tag{33}$$

In Equation (32), Cleaver and Yates assumed

$$\alpha = 0.067 \frac{u^{*2}}{\nu} \tag{34}$$

so that

$$v^{f+} = \frac{1}{2} \text{ at } y^+ = 10. \tag{35}$$

Evaluating Equations (30) and (31), and solving for the limiting trajectory, it follows that

$$\ln\frac{z^+}{z_0} = \int_{\sqrt{\frac{\alpha\nu}{u^{*2}}}y_0^+}^{\sqrt{\frac{\alpha\nu}{u^{*2}}}y^+} \{\frac{\varphi' - \tau^+(\frac{\alpha\nu}{u^{*2}})(\varphi'^2 - \varphi\varphi'')}{\varphi + \tau^+(\frac{d\nu}{u^{*2}})\varphi\varphi'}\}dy. \tag{36}$$

For the boundary condition at the wall for the limiting trajectory, Cleaver and Yates assumed

$$y^+ = \frac{d^+}{2} \qquad \text{at} \qquad z^+ = 70. \tag{37}$$

(Note that the value $z^+ = 70$ is too high. The correct boundary condition is $z^+ = 25.$) When z_o^+ is known, then

$$A_c = \frac{z_0^+}{z^+}. \tag{38}$$

Cleaver and Yates used Laufer's data near the wall and found

$$u_D^+ = \frac{9}{400}\frac{\rho^f}{\rho^p}\tau^+ \exp\{0.48\tau^+\} \qquad \text{for} \qquad \tau^+ << 1 \tag{39}$$

$$u_D^+ = 0.45\exp\{-\frac{\tau}{0.9}\int_{d^+/2}^{\infty} 1 - \frac{f(y)}{0.9})dy\} \qquad \text{for} \qquad \tau^+ >> 1 \tag{40}$$

Note that A_c varies with y_0^+, and $y_0^+ = 10$ was used by Cleaver and Yates. They also argued that a large correction factor is needed to account for the convection effects that are neglected. This lead to

$$u_D^+ = 8.5A_c. \tag{41}$$

For the diffusion range, Cleaver and Yates suggested

$$u_D^+ = 0.084 S_c^{-2/3}. \tag{42}$$

Alternatively, Chamberlain suggested

$$u_D^+ = \frac{u^*}{u_m} S_c^{-2/3}, \quad \frac{u^*}{u_m} \sim 0.047 \sim 0.067. \tag{43}$$

Using (41) and (42), the minimum deposition rate occurs at

$$\tau^+ S_c^{2/3} = 0.069 \frac{\rho_p}{\rho_f}. \tag{44}$$

Combing the effects of inertial and Brownian, the model equation of Cleaver and Yates is given by Equation (23). The predicted deposition rates for a range of density ratios are shown in Figure 9, and are compared with other models.

Fichman et al., J. Aerosol Sci. 19, 123 (1988)

Fichman et al. (1988) used the model of Cleaver and Yates, but included the lift force effect. In addition, they fit semi-analytical expression to the velocity field for different range of distances near the wall. Accordingly

$$U^+ = y^+ \tag{45}$$

$$\left.\begin{aligned} v^+ &= B\phi = 0.625 B^3 y^{+2} \\ \phi &= 0.625\eta^2, \quad \eta = By^+, \qquad B = 0.271 \end{aligned}\right\} \text{for } y^+ \le 2, \tag{46}$$

$$\left.\begin{aligned} v^+ &= c\phi = 0.24c - 0.71c^2 y^+ \\ \phi &= 0.71\eta - 0.24, \qquad \eta = cy^+, \qquad c = 0.174 \end{aligned}\right\} \text{for } 2 \le y^+ \le 7, \tag{47}$$

$$\left.\begin{aligned} U^+ &= 0.3y^+ + 0.5 \\ v^+ &= c\phi = 0.6c - c^2 y^+, \ \phi = \eta - 0.6 \end{aligned}\right\} \text{for } 7 \le y^+ \le 30. \tag{48}$$

The particle flux to the wall then is given by

$$u_D^+ = \frac{1}{2} A_c v_0^+, \tag{49}$$

where v_0^+ is the downsweep velocity and

$$A_c = \frac{z_{lim}}{\Lambda/4} = \frac{z^+_{lim}}{\Lambda^+/4}. \tag{50}$$

The corresponding deposition velocity is then given as

$$u^+_D = \frac{2z^+_{lim}v^+_0}{\Lambda^+}, \tag{51}$$

and z_{lim} is the distance from the centerline.

The equations of motion including the drag and lift forces are:

$$\tau^+ \frac{d^2x^+}{dt^{+2}} = U^+ - \frac{dx^+}{dt}, \tag{52}$$

$$\tau^+ \frac{d^2y^+}{dt^{+2}} = v^+ - \frac{dy^+}{dt} + K\left(U^+ - \frac{dx^+}{dt}\right), \tag{53}$$

$$\tau^+ \frac{d^2z^+}{dt^{+2}} = w^+ - \frac{dz^+}{dt}. \tag{54}$$

where

$$K = \tau^+ L^+,\ L^+ = \frac{L\nu}{u^{*2}}, \tag{55}$$

$$L \approx \frac{6.46\mu\left(\frac{d}{2}\right)^2}{\nu^{\frac{1}{2}}m_p}\left(\frac{dU}{dy}\right)^{\frac{1}{2}} = \frac{3.08\mu\dot{\gamma}^{\frac{1}{2}}}{\nu^{1/2}d\rho_p}, \quad \text{with} \quad \dot{\gamma} = \frac{dU}{dy}, \tag{56}$$

For small stopping distance with $s^+ \le 2$, Fichman et al. (1988) found that

$$\frac{4z^+_{lim}}{\Lambda^+} = \frac{\frac{d^2}{4} + \left(d^+ + s^+\right)s^+}{4}, \tag{56}$$

where the modified stopping distance is given as

$$s^+ = \frac{L^+\tau^{+2}\left(u_{po}^+ - \dot{\gamma}^+ y_0^+\right) + \tau^+ v_{po}^+}{1 - \tau^{+2} L^+ \dot{\gamma}^+},$$

For $s^+ \geq 2$, no closed form solution is available and they used a numerical simulation procedure for effective evaluation of the deposition velocity.